

# **The Fatigue Design of Electrical Spot Weldments**

by

**M. H. Swellam, G. Banás, and F. V. Lawrence**

A report of

**MATERIALS ENGINEERING MECHANICAL BEHAVIOR**  
**College of Engineering, University of Illinois at Urbana-Champaign**

**August 1993**

# THE FATIGUE DESIGN OF ELECTRICAL RESISTANCE SPOT WELDMENTS

by

M. H. Swellam, G. Banaś, F. V. Lawrence  
University of Illinois at Urbana-Champaign

## Summary

A general parameter ( $K_i$ ) is proposed which reflects the magnitude of the stress field at the periphery of the spot weld and which correlates the fatigue behavior of all spot weld geometries in terms of normal, shear, and bending forces ( $P$ ,  $Q$  and  $M$ ) applied to the weldment. The  $K_i$  is an empirically derived quantity which is based on the concepts of mixed mode fracture mechanics and experimental data. The  $K_i$  parameter allows the engineer to predict the fatigue behavior for any spot weld for which the applied maximum values of the loads  $P$ ,  $Q$  and  $M$  are known from experiment or global structural analysis. Examples of the application of  $K_i$  to spot-weld fatigue design are given.

## DEFINITION OF SYMBOLS USED

Symbol	Definition
CP	Coach peel spot weld geometry
CT	Cross tension spot weld geometry
D	Nugget Diameter
DS	Double shear spot weld geometry
e	Load eccentricity relative to nugget center or periphery
F	Remotely applied load
$F_{\max}$	Maximum value of the remotely applied load
HSLA	High strength low alloy steel
$K_i$	Fatigue spot weld design parameter
$\bar{K}_i$	Mean value of stress index
$K_I$	Mode I (opening mode) stress intensity factor
$K_{II}$	Mode II (in-plane shear mode) stress intensity factor
LC	Low carbon steel
M	Bending moment transmitted by the nugget ( $M = F e$ )
$N_f$	Fatigue life (either to complete separation or visible crack)
$N_I$	Stage I of fatigue life (initiation)
$N_{II}$	Stage I + Stage II of fatigue life (initiation + propagation of crack through the thickness of plate)
P	Normal component of applied load transmitted by the nugget
Q	Shearing component of the applied load transmitted by the nugget
R	Load ratio ( $F_{\min}/F_{\max}$ )
STT	Sheet to tube weldment geometry
t	Sheet thickness
TS	Tensile shear spot weld geometry
W	Sheet width or spacing between nuggets
$\beta$	Material parameter (2 for LC and 3 for HSLA)
$\theta$	Flange angle of a coach-peel joint

## ABSTRACT

Initial stress intensity factors,  $K_I$  and  $K_{II}$ , for a semi-infinite geometry were used to calculate an equivalent stress intensity factor ( $K_{eq}$ ). The equivalent stress intensity factor was subsequently modified to the stress index ( $K_i$ ) to account for the finite geometry and mean stress effects on the total fatigue life. The stress index ability to correlate the fatigue data of different spot welded joints was validated and subsequently best-fit equations were generated.

## 1. THE EQUIVALENT STRESS INTENSITY FACTOR FOR SPOT WELDMENTS

Figure 1 compares the fatigue performance of double-shear, tensile-shear and coach-peel joints of low carbon and HSLA steels. The relatively poor performance of the coach-peel specimens is attributed to a difference in the nature of the loads transferred through the nugget. While the spot weld in a double-shear specimen is subjected mainly to shear loads, that of coach-peel specimen is subjected to axial loads and moments. The spot weld in the tensile-shear specimen is mainly subjected to a combination of shear and bending moments. As depicted in Fig. 1, the applied load fails to correlate the fatigue data of different spot welded geometries.

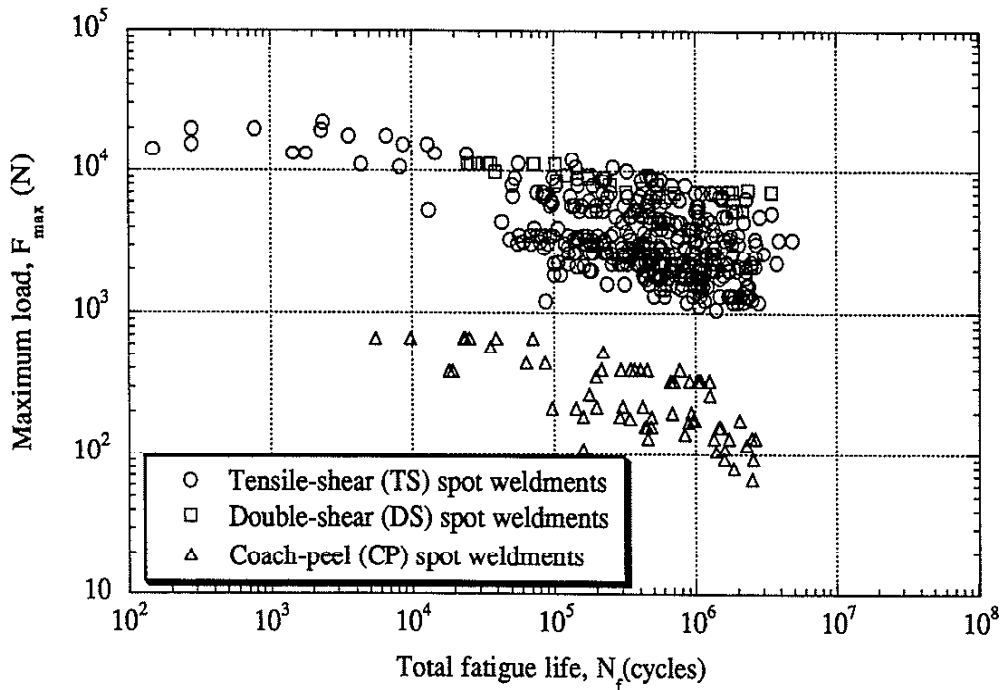


Fig. 1 Maximum applied load vs. total fatigue life for different DS, TS and CP specimens [1].

Figure 2 shows one-half of a spot weld subjected to arbitrary load ( $F$ ) at an angle ( $\theta$ ) to the sheets interface. Because of the eccentricity of the loading ( $e$ ), the nugget experiences a normal force ( $P$ ) a shearing force ( $Q$ ) and an applied moment ( $M = F * e$ ). In general, a spot weld nugget could be subjected to a combination of axial loads ( $P$ ), shearing loads ( $Q$ ), and bending moments ( $M$ ), that is a combination of Modes I and II.

Approximate mode I and II stress intensity factors associated with the semi-infinite connection subjected to an axial load (P), shear load (Q) and moment (M) are calculated by linear superposition as follows [2]:

$$K_I = K_{\text{axial}} + K_{\text{moment}} \quad (1)$$

$$K_{II} = K_{\text{shear}} \quad (2)$$

$$K_{\text{axial}} = \frac{P}{D\sqrt{\pi \frac{D}{2}}} \quad (3)$$

$$K_{\text{moment}} = \frac{6M}{D^2\sqrt{\pi \frac{D}{2}}} \quad (4)$$

$$K_{\text{shear}}^* = \frac{Q}{D\sqrt{\pi \frac{D}{2}}} \quad (5)$$

where:

- D = Nugget diameter
- P = Normal component of the applied load: see Fig. 2
- Q = Shearing component of the applied load
- M =  $F \cdot e$
- e = Eccentricity of loading

The equivalent stress intensity factor which reflects the notch root stresses (and thus the incidence of fatigue there) is subsequently calculated from the stress intensity factors for the semi-infinite joint along the centerline of the weld nugget. Through a simplified form of Broek's Mode I equivalent stress intensity factor [3], the initial equivalent Mode I stress intensity factor ( $K_{Ieq}$ ) for the semi-infinite spot weld joint is calculated from:

$$K_{Ieq} = \sqrt{K_I^2 + \beta K_{II}^2} \quad (6)$$

where  $\beta$  is a constant which reflects the material response to Mode II as well as the effect of the residual stress state at the notch tip. Different materials and different residual stress states

\* The  $K_{II}$  value for a direct shear force is approximated by the  $K_{III}$  value induced by a torque. In both cases the nugget is subjected to shear stresses.

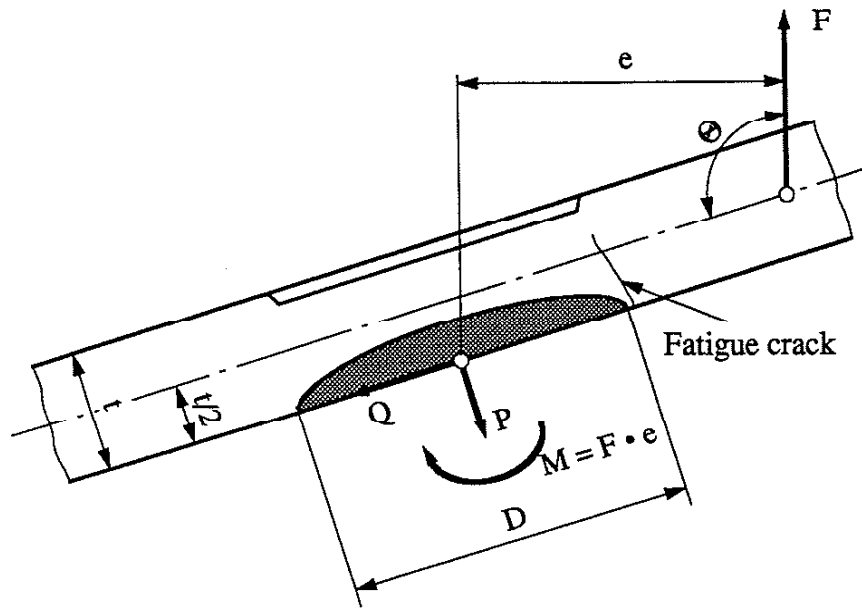


Fig. 2 Force components  $P$ ,  $Q$  and  $M$  resulting from a general applied load ( $F$ ) transmitted across the weld nugget of an electrical resistance spot weldment.

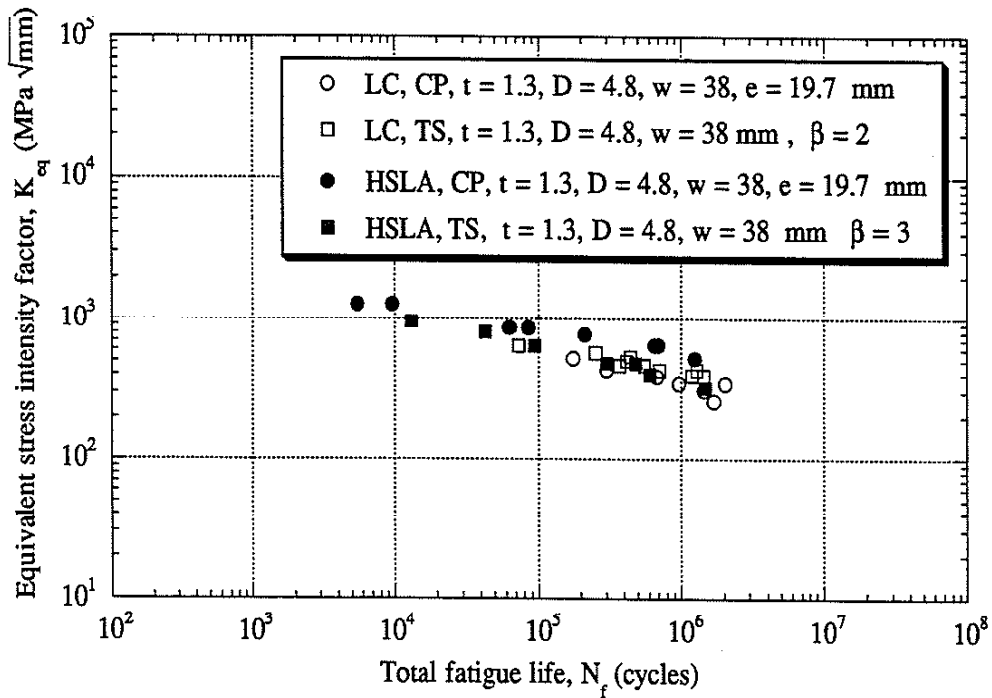


Fig. 3  $K_{eq}$  and Load - Life presentation of total fatigue life data for tensile-shear and coach-peel [4] low carbon ( $\beta = 2$ ) and HSLA ( $\beta = 3$ ) specimens.

would yield different values of  $(\beta)$ . The constant  $(\beta)$  was obtained by collapsing two sets of total fatigue life data for specimens with the same sheet thickness, nugget diameter and specimen width. The first set of data was for coach-peel specimens (Mode I only) while the second was for tensile-shear specimens (Modes I and II). Values of  $(\beta)$  obtained in this study from data in reference [5] were 2 and 3 for the LC and HSLA specimens respectively as shown in Fig. 3.

## 2. EFFECTS OF FINITE GEOMETRY

The  $(K_{I_{eq}})$  was derived to collapse the fatigue data of tensile-shear and coach-peel specimens of the same sheet thickness, nugget diameter and specimen width. However, when the  $(K_{I_{eq}})$  was used to correlate the fatigue data of tensile-shear specimens with different nugget diameter, sheet thickness and specimen width, a wider scatter (relative to the applied load-life data presentation) was observed: see Fig. 4. The  $(K_{I_{eq}})$  failed to correlate the fatigue data of tensile-shear specimens with different dimensions; it exaggerates the effect of the nugget diameter and fails to account for the variation in the sheet thickness and specimen width. The reason for this failure is attributed to two main reasons: firstly, the  $K_I$  and  $K_{II}$  solutions of the

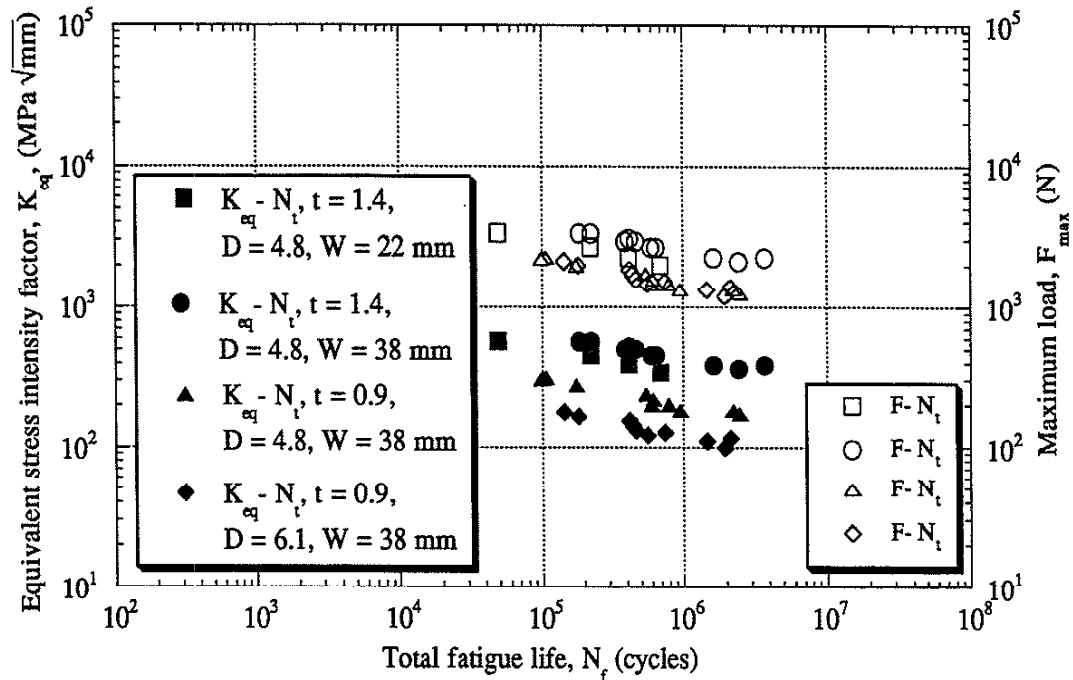


Fig. 4  $K_{eq}$  and Load - Life presentation of total fatigue life data for tensile-shear low carbon specimens [5],  $R = 0$ .



spot welded semi-infinite joint do not reflect the effects of the finite dimensions on the fatigue life; and secondly, the initial stress intensity factors reflect the initial stress and strain states at the notch tip but not the progressive nature of the fatigue crack.

As shown in Fig. 5, the fatigue strength (at  $10^5$  cycles) changes linearly with the sheet thickness; the (0.0, 0.0) data point is a fictitious point which has to be satisfied by the linear relation as much as possible. Similarly, the effect of the specimen width is depicted in Fig. 6; the relation between the fatigue strength and the specimen width can be represented by a power function with an exponent equal to 0.49.

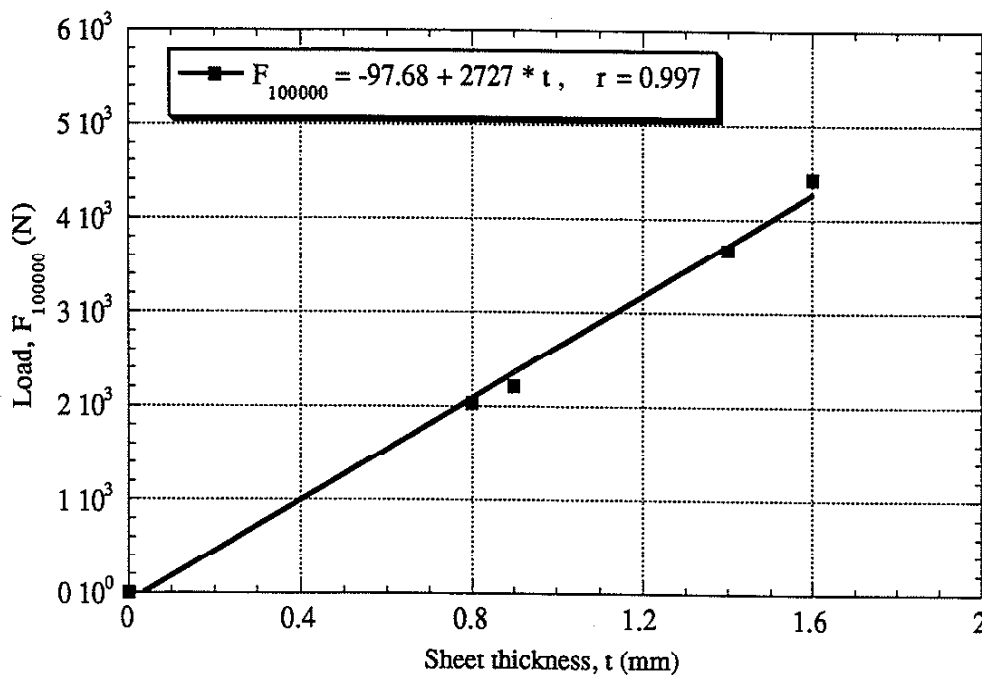


Fig. 5 Sheet thickness effect on the fatigue strength at  $10^5$  cycles [5].

Based upon these two functional forms and the weak dependence of the fatigue life on the nugget diameter [5], the fatigue data of Fig. 4 are replotted in terms of the  $(F/(t\sqrt{W}))$  factor in Fig. 7. The  $(F/(t\sqrt{W}))$  factor, which possesses the units of the stress intensity factor, collapsed the data into a narrow band.

In order to incorporate the above effects of the geometrical dimensions ( $t$ ,  $W$  and  $D$ ) on the fatigue life, the  $(K_{Ieq})$  (Eq. 6) for a tensile-shear specimen can be expanded

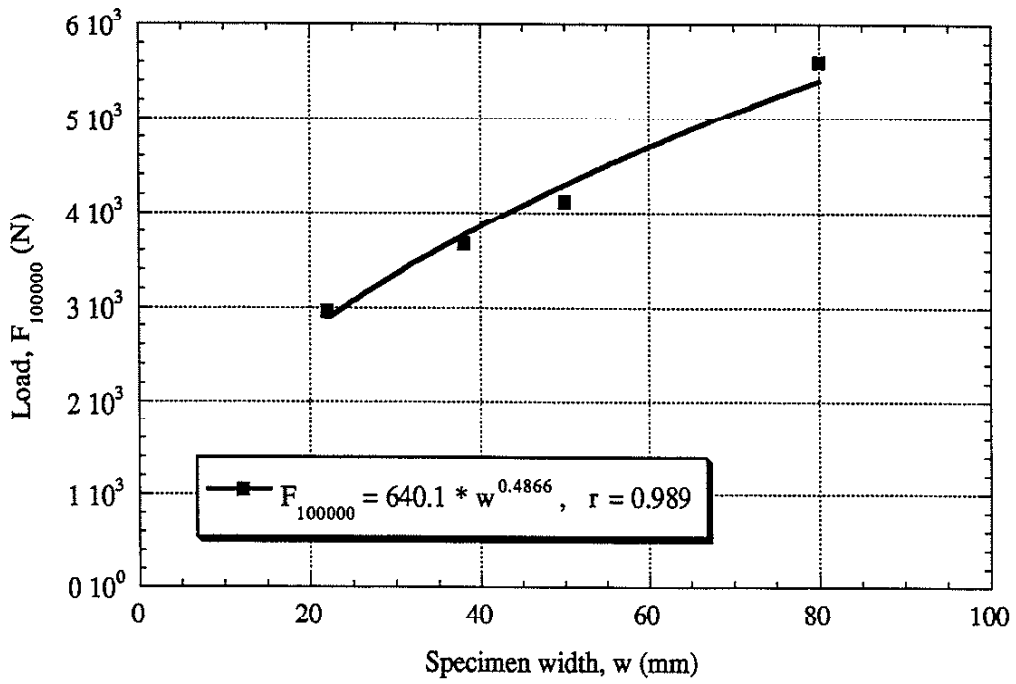


Fig. 6 Specimen width effect on the fatigue strength at  $10^5$  cycles [5].

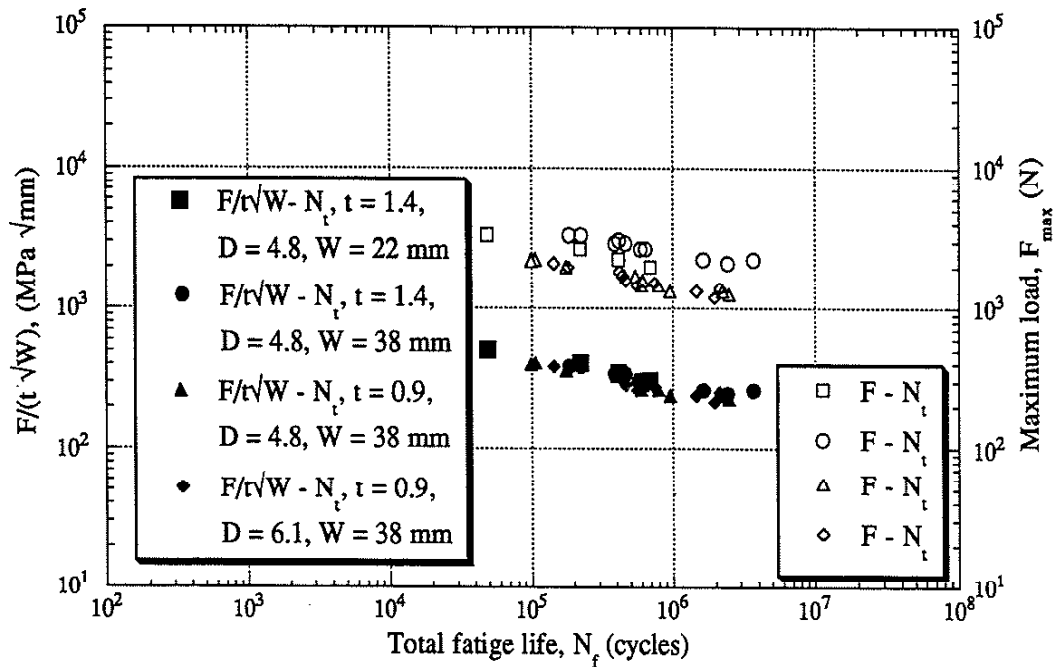


Fig. 7  $F/(t\sqrt{W})$  and load-life presentation of total fatigue life data for low carbon tensile-shear specimens [5],  $R = 0$ .

$$K_{Ieq} = \sqrt{K_I^2 + \beta K_{II}^2} = \frac{F}{D\sqrt{\pi \frac{D}{2}}} \sqrt{\left(\frac{3t}{D/2}\right)^2 + \beta} \quad (7)$$

and divided by a geometrical correction factor (G) given by

$$G = \sqrt{\frac{8t^2W}{D^3} \left(\frac{36t^2}{D^2} + 1\right)} \quad (8)$$

The key points in determining the G factor were to account for the different modes of deformation and at the same time maintain the  $\frac{F}{t\sqrt{W}}$  form in the case of tensile-shear specimens. Subsequently, the  $K_{i \max}$  parameter can be expressed as follows

$$K_{i \max} = \frac{K_{Ieq}}{G} = \sqrt{\frac{K_I^2 + \beta K_{II}^2}{\frac{8t^2W}{D^3} \left(\frac{36t^2}{D^2} + 1\right)}} \quad (9)$$

### 3. EFFECT OF MEAN STRESS

Furthermore, three sets of tensile-shear specimens loaded with  $R = -0.2$ ,  $R = 0$  and  $R = 0.5$  [5] were used to determine the R-ratio effect. Four different parameters ( $K_{i \max}$ ,  $\Delta K_i = K_{i \max} * (1 - R)$ ,  $(\Delta K_i * K_{i \max})^{0.5}$  and  $K_{i \max} * (1 - R)^{0.85}$ ) were used to correlate the total fatigue life data of the considered load sets. The least scatter in the data was observed in the case of  $K_{i \max} * (1 - R)^{0.85}$  [5]. Hence, the final form for the ( $K_i$ ) parameter is as follows:

$$K_i = \sqrt{\frac{K_I^2 + \beta K_{II}^2}{\frac{8t^2W}{D^3} \left(\frac{36t^2}{D^2} + 1\right)}} (1-R)^{0.85} \quad (10)$$

### 4. VALIDATION OF $K_i$ AS A UNIFIED PARAMETER FOR CORRELATING FATIGUE DATA

HSLA and low carbon double-shear, tensile-shear and coach-peel total fatigue life data are correlated in terms of the ( $K_i$ ) in Fig. 8. The ( $K_i$ ) collapsed the data into a narrow band

despite the differences in specimen type. Three best-fit equations are generated; one for the HSLA data, the second for the low carbon data, and the third for the combined HSLA and low carbon data. As shown in Fig. 8, the best-fit lines lie close to each other.

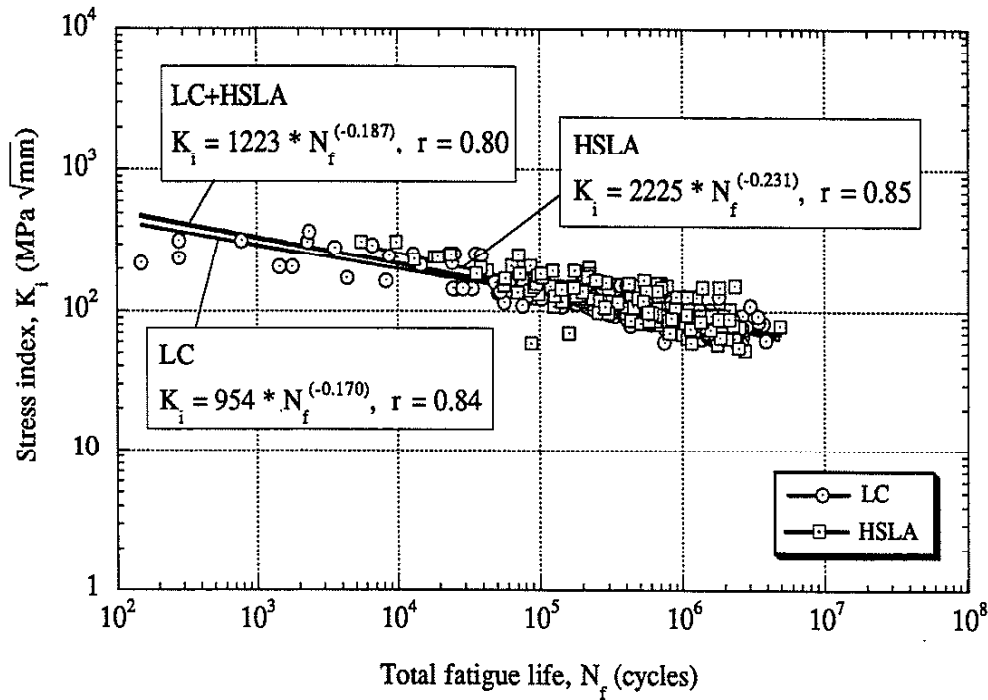


Fig. 8 Stress index ( $K_i$ ) versus total fatigue life for double shear, tensile shear and coach peel specimens [1].

Figures 9 and 10 shows that the ( $K_i$ ) parameter can also be used to correlate the fatigue data of other spot welded geometries. Fatigue data of channel to channel (Davidson's specimen [6-8] and sheet to channel (Stanford's specimen [9]) were also collapsed into a narrow band which agrees well with the best-fit equation generated in Fig. 8. Cross tension, tensile shear sheet-to-tube and cross tension sheet-to-tube also agree well with the best fit equation of Fig. 8 as shown in Fig. 10.

Figure 11 presents the Stage I fatigue data for all the tensile-shear specimens monitored by the potential drop technique [5]. Three best-fit equations were generated for the HSLA and the low carbon data separately and combined; the best-fit lines lie close to each other especially in the long life regime where most of the data points fall. A similar plot and best-fit equation

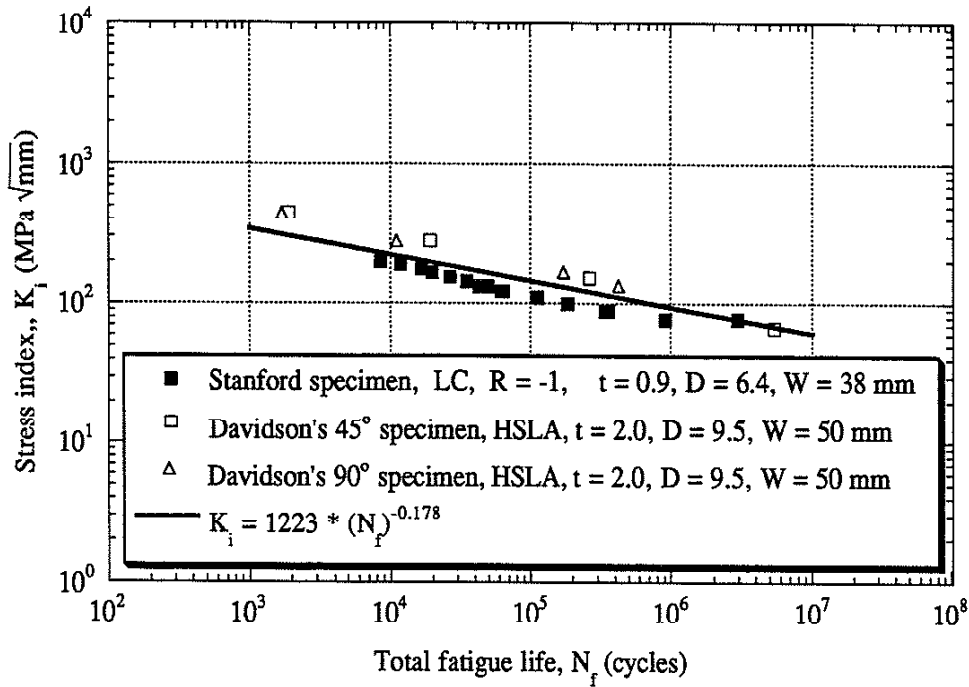


Fig. 9  $K_i$  vs. total fatigue life for Stanford's [9] sheet to channel specimen and Davidson's [6-8] channel to channel specimens.

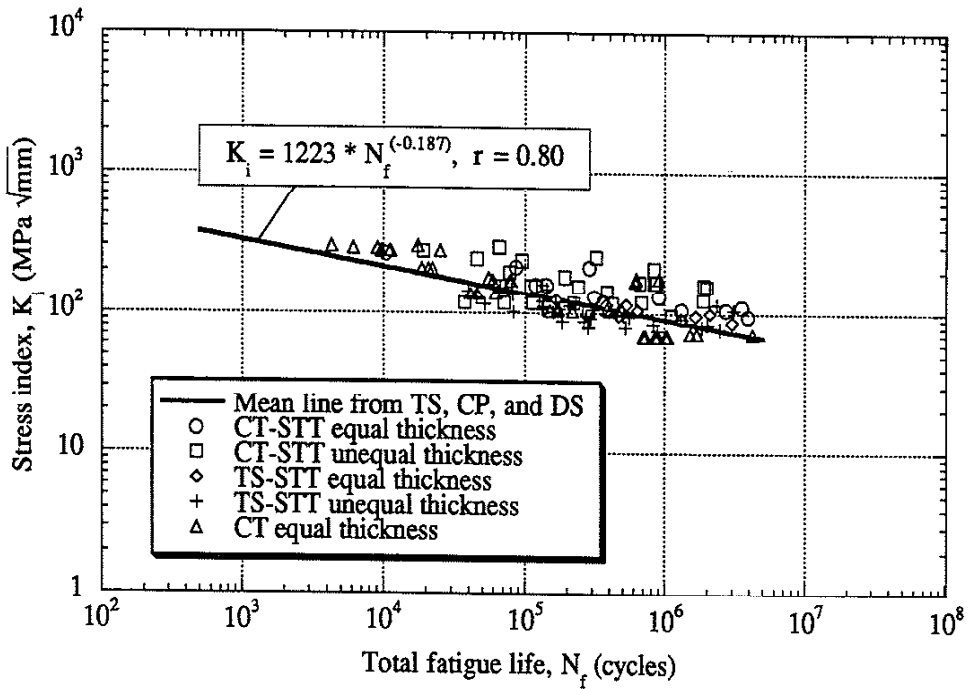


Fig. 10  $K_i$  vs. total fatigue life for cross tension, tensile shear sheet-to-tube and cross tension sheet-to-tube specimens.

for the fatigue life up to the first occurrence of a fatigue crack on the outer surface of the tensile shear specimen is shown in Fig. 12. Figure 13 shows the ( $K_i$ ) versus total fatigue life up to complete separation.

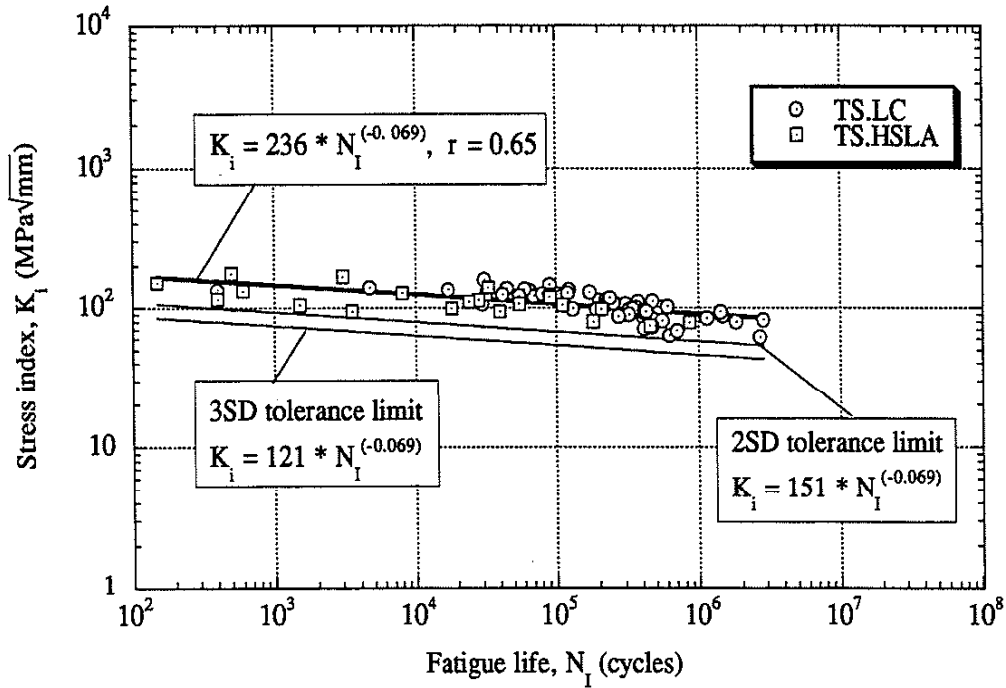


Fig. 11  $K_i$  vs. Stage I (Initiation Only) fatigue data for HSLA and low carbon tensile-shear specimens [5].

Assuming a log-normal distribution of fatigue data points generated for the entire range of stress index ( $K_i$ ), a power relationship between the stress index ( $K_i$ ) and the fatigue life ( $N$ ) can be fitted to the data. The power function as shown in Fig. 8 and Figs. 10-13 is of the form:

$$\log K_i = A + B \log N \quad (11)$$

where (A) and (B) in Eq. 11 were determined using the least square method [11] under the following assumptions:

- all fatigue lives ( $N$ ) are independent,
- there are neither run-outs nor suspended tests,

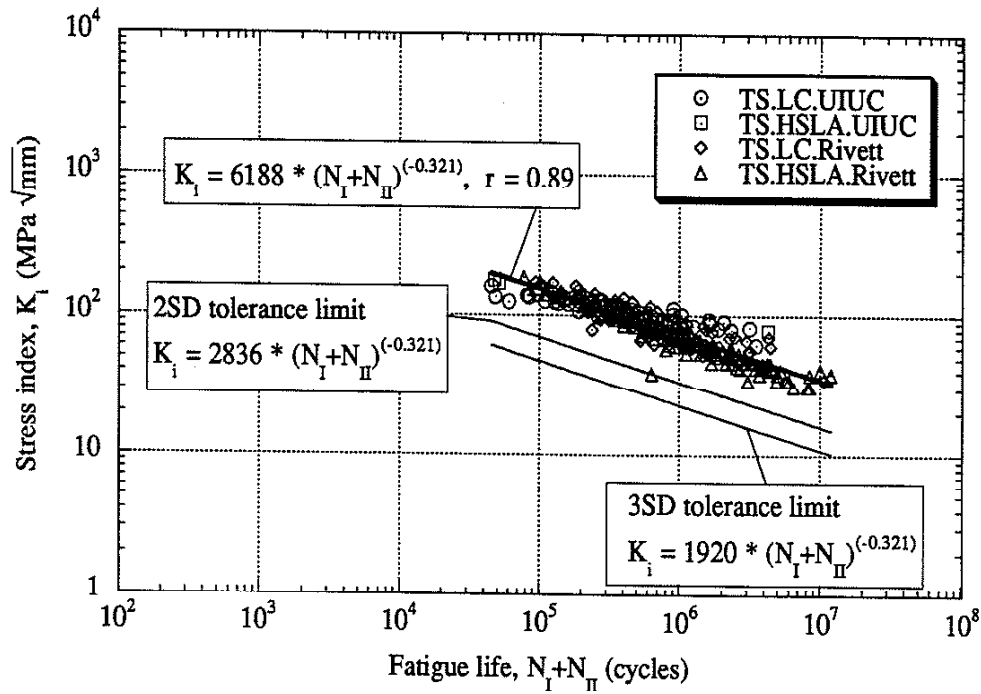


Fig. 12  $K_i$  vs. Fatigue Life up to the first occurrence of a fatigue crack on the outer surface of the tensile shear specimen [5, 10].

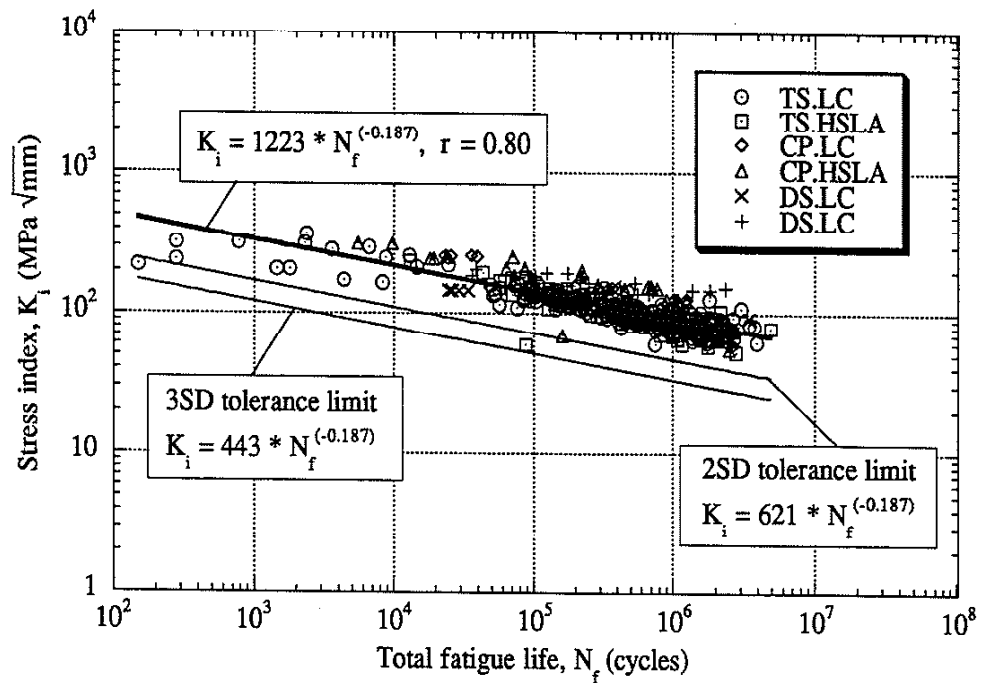


Fig. 13  $K_i$  vs. Fatigue Life up to complete separation of different spot welded specimens [2].

- variance of the log-normal distribution is constant.

Equation 11 allows to calculate a mean value of ( $K_i$ ) for given fatigue life with 50% probability that the test specimens will survive under the applied load. For design purposes, either two standard deviation (2SD) or three standard deviation (3SD) confidence limit is recommended. Figures 11-13 comprise one-sided tolerance limits calculated using the formula:

$$\log K_{i(2SD)} = \log \bar{K}_i - 2SD \quad (12)$$

$$\log K_{i(3SD)} = \log \bar{K}_i - 3SD \quad (13)$$

where:

$\bar{K}_i$  - is the mean value of stress index

SD - is the standard deviation calculated from:

$$SD = \sqrt{\frac{\sum(\log K_i - \log \bar{K}_i)^2}{n - 2}} \quad (14)$$

where:

n - is the number of test data points.

One-sided tolerance limit could be used in design with either 2SD or 3SD confidence level that a particular spot weld will not fail under applied load level and for specified number of cycles.

## 5. SUMMARY

The ( $K_i$ ) parameter collapsed the total fatigue life data of double-shear, tensile-shear and coach-peel specimens into a narrow band; it considered the different modes (Mode I and II) at the edge of the spot weld, the difference in the fatigue response of HSLA and low carbon specimens, and the different geometrical dimensions.

The ( $K_i$ ) parameter provides the designer with a useful tool for determining the fatigue life of different spot-welded joints. Moreover, the ( $K_i$ ) parameter helps the designer determine and compare the effects of several variables on the fatigue performance of the joints without having to resort to extensive testing as shown in the report.



## 6. REFERENCES

1. Fatigue Data Bank for Spot welds at the University of Illinois.
2. Tada, H., Paris, P. and Irwin, G., "The Stress Analysis of Cracks Handbook", Del Research Corporation, 1985.
3. Broek, D., Elementary Engineering Fracture Mechanics, Fourth Edition. 1984.
4. Unpublished spot weld fatigue test data of the authors.
5. Swellam, M. H. and Lawrence, F. V. "A Fatigue Design Parameter for Spot Welds", Fracture Control Program Report No. 157, University of Illinois, 1991.
6. Davidson, J. A. and Imhof, E. J., "A Fracture-Mechanics and System-Stiffness Approach to Fatigue Performance of Spot-Welded Sheet Steels", SAE technical report No. 830034 Detroit, Michigan, 1983.
7. Davidson, J. A. and Imhof, E. J., "The Effect of Tensile Strength on the Fatigue Life of Spot-Welded Sheet Steels", SAE technical report No. 840110. Detroit, Michigan, 1984.
8. Davidson, J. A., "A Review of the Fatigue Properties of Spot- Welded Sheet Steels.", SAE technical report No. 830033 Detroit, Michigan 1983.
9. Personal communication with Prof. Sherri Sheppard, Mechanical Engineering Department, Stanford University, California.
10. Rivet, R. M. " Assessment of Single Resistance Spot Welds in Low Carbon and High Strength Steel Sheet - Part 2 Fatigue and Impact Properties " The Welding Institute research report No. 212/1983.
11. Harnett, D.L., " Introduction to Statistical Methods ", Addison-Wesley Publishing Company, 1975.

**APPENDIX A**

**THE DEVELOPMENT OF A UNIFIED PARAMETER FOR SPOT WELDS  
THE STRESS INDEX ( $K_I$ )**

By

M .H. Swellam

G. Banaś

F. V. LAWrence

University of Illinois at Urbana-Champaign

## DEFINITION OF SYMBOLS USED

Symbol	Definition
CP	Coach peel spot weld geometry
CT	Cross tension spot weld geometry
D	Nugget Diameter
DS	Double shear spot weld geometry
e	Load eccentricity relative to nugget center or periphery
F	Remotely applied load
F <sub>max</sub>	Maximum value of the remotely applied load
HSLA	High strength low alloy steel
K <sub>i</sub>	Fatigue spot weld design parameter
K <sub>I</sub>	Mode I (opening mode) stress intensity factor
K <sub>II</sub>	Mode II (in-plane shear mode) stress intensity factor
LC	Low carbon steel
M	Bending moment transmitted by the nugget ( $M = F e$ )
N <sub>f</sub>	Fatigue life (either to complete separation or visible crack) (cycles)
P	Normal component of applied load transmitted by the nugget
Q	Shearing component of the applied load transmitted by the nugget
R	Load ratio ( $F_{min}/F_{max}$ )
STT	Sheet to tube weldment geometry
t	Sheet thickness
TS	Tensile shear spot weld geometry
W	Sheet width or spacing between nuggets
$\beta$	Material parameter (2 for LC and 3 for HSLA)
$\theta$	Flange angle of a coach-peel joint

## 1. THE FATIGUE BEHAVIOR OF ELECTRIC RESISTANCE SPOT WELDS

The fatigue behavior of electric resistance spot welds is generally determined using laboratory specimens such as the double-shear (DS), tensile-shear (TS), coach-peel (CP) and others which roughly approximate common service conditions: see Table 1. Each of the different spot weld geometries has its own characteristic load-life fatigue curve (see Fig. 1) because the geometry and loads applied to the weld differs from one geometry to another.

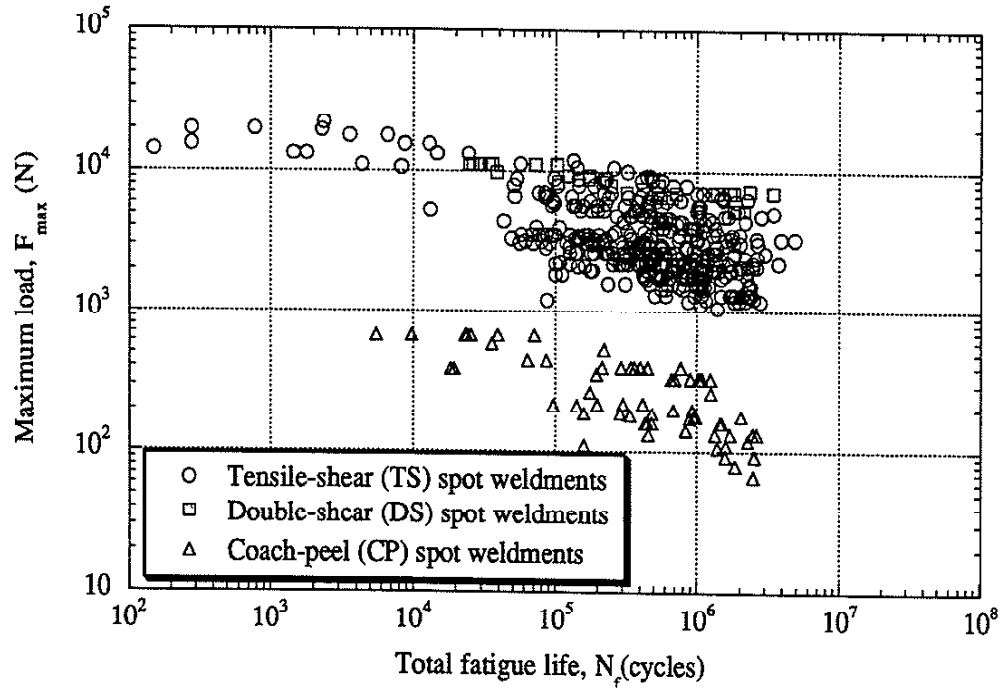


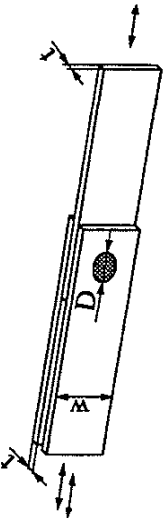
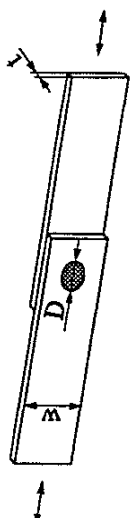
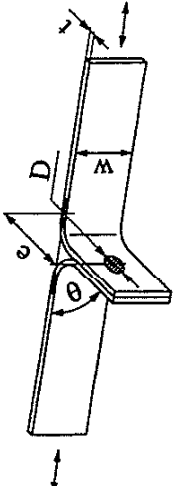
Fig. 1 Maximum applied load versus total fatigue life ( $N_f$ ) for different DS, TS and CP specimens [1].

## 2. THE $K_i$ PARAMETER

The weld nugget itself is the same for all the different geometries shown in Table 1. What differs from geometry to geometry is the nature of the stresses (or modes of deformation) generated at the periphery of the weld nugget by the normal loads ( $P$ ), shearing loads ( $Q$ ) and bending moments ( $M$ ) applied to the joint: see Table 1. This condition has led to the development of a parameter ( $K_i$ ) which is an index of the stress field at the periphery of the spot weld and which, as will be shown, correlates the fatigue behavior of all spot weld geometries in terms of the average normal, shear and bending forces ( $P$ ,  $Q$  and  $M$ ) applied to the weldment: see Table 1. The  $K_i$  parameter is an empirically derived quantity based on the concepts of mixed-mode fracture mechanics and the available experimental data [2,3]:

Table 1

GEOMETRY AND LOAD COMPONENTS OF COMMON SPOT WELDMENTS

Geometry	Load Components for Eq. 1			Simplified Expression for $K_1$ ( $R = 0$ )
	P	Q	M	
 <p>Double Shear (DS)</p>	0	$\frac{F}{2}$	0	$K_1 = \frac{F}{4t\sqrt{\pi W(36t^2 + D^2)}} D \sqrt{\beta}$
 <p>Tensile Shear (TS)</p>	0	F	Ft	$K_1 = \frac{F}{2t\sqrt{\pi W(36t^2 + D^2)}} \sqrt{36t^2 + \beta D^2}$
 <p>Coach Peel (CP), <math>\theta = 90^\circ</math></p>	F	0	Fe	$K_1 = \frac{F}{2t\sqrt{\pi W(36t^2 + D^2)}} (D + 6e)$

"e" is the distance between the line of load application and the center of the weld

Table 1 (Cont'd)

GEOMETRY AND LOAD COMPONENTS OF COMMON SPOT WELDMENTS

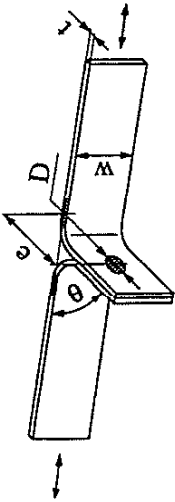
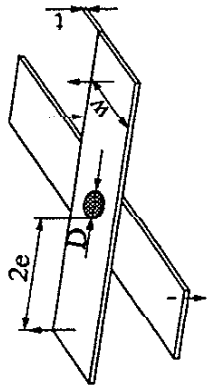
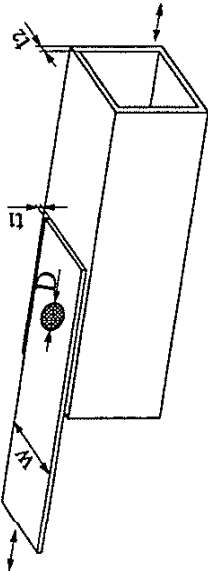
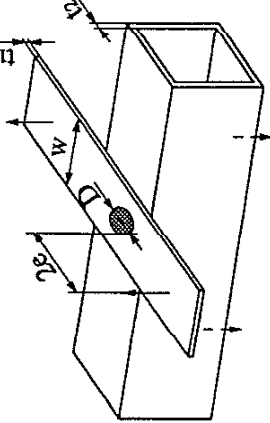
Geometry	Load Components for Eq. 1			Simplified Expression for $K_1$ ( $R = 0$ )
	P	Q	M	
 <p>Coach-Peel with general flange angle (<math>\theta</math>)</p> <p>"e" is the distance along the flange between the line of load application and the center of the weld.</p>	$F \sin \theta$	$F \cos \theta$	$F e \sin \theta$	$K_1 = \frac{F_{\max}}{2t\sqrt{\pi W(36t^2 + D^2)}} \sqrt{(D + 6e)^2 \sin^2 \theta + \beta D^2 \cos^2 \theta}$
 <p>Cross Tension (CT)</p> <p>Each of the indicated forces is equal to half the total applied force (F)</p>	F	0	$\frac{Fe}{2}$	$K_1 = \frac{F}{2t\sqrt{\pi W(36t^2 + D^2)}} (D + 3e)$

Table 1 (Cont'd)

GEOMETRY AND LOAD COMPONENTS OF COMMON SPOT WELDMENTS

Geometry	Load Components for Eq. 1			Simplified Expression for $K_i$ ( $R = 0$ )
	P	Q	M	
 <p><b>Tensile Shear Sheet-to-Tube (TS-STT)</b></p>	0	F	$\approx 0$	$K_i = \frac{F}{2t\sqrt{\pi W(36t^2 + D^2)}} D \sqrt{\beta}$
 <p><b>Cross Tension Sheet-to-Tube (CS-STT)</b></p> <p>Each of the indicated forces is equal to half the total applied force (F)</p>	F	0	$\frac{Fe}{2}$	$K_i = \frac{F}{2t\sqrt{\pi W(36t^2 + D^2)}} (D + 3e)$

$$K_i = (1-R)^{0.85} \sqrt{\frac{K_{I \max}^2 + \beta K_{II \max}^2}{\frac{8t^2W}{D^3} \left( \frac{36t^2}{D^2} + 1 \right)}} \quad (1)$$

where:

$$K_I = K_{\text{axial}} + K_{\text{moment}} = \frac{P}{D\sqrt{\pi D/2}} + \frac{6M}{D^2\sqrt{\pi D/2}}$$

$$K_{II} = K_{\text{shear}} = \frac{Q}{D\sqrt{\pi D/2}}$$

$\beta$  = Material parameter (2 for low carbon (LC) and 3 for high strength low alloy (HSLA) steel sheet [2,3]).

The above form of Eq. 1 is slightly different from that reported in the earliest descriptions of  $K_i$  [2,3]; the current form leads to better correlations with experimental data. Simplified forms of the expression for  $K_i$  are given below for the many of the geometries included in Table 1. See Table 1 for the definition of the geometric parameters  $D$ ,  $W$ , and  $t$  and load application for each geometry.

Double-shear (DS) specimen (R = 0)

$$K_i = \frac{F}{4t\sqrt{\pi W(36t^2+D^2)}} D \sqrt{\beta} \quad (2)$$

Tensile-shear (TS) specimen (R = 0)

$$K_i = \frac{F}{2t\sqrt{\pi W(36t^2+D^2)}} \sqrt{36t^2 + \beta D^2} \quad (3)$$

Coach-peel (CP) specimen (R = 0)

$$K_i = \frac{F}{2t\sqrt{\pi W(36t^2+D^2)}} (D + 6e) \quad (4)$$

Cross-Tension (CT) specimen (R = 0)

$$K_i = \frac{F}{2t\sqrt{\pi W(36t^2+D^2)}} (D + 3e) \quad (5)$$



### 3. CORRELATION OF $K_i$ WITH EXPERIMENTAL DATA

#### 3.1 $K_i$ as a function of fatigue life ( $N_f$ )

In Fig. 2,  $K_i$  is seen to provide an excellent correlation with the fatigue data of 482 spot welds having DS, TS and CP geometries [1]. Thus, the parameter  $K_i$  is a unifying concept which allows the engineer to predict the fatigue behavior for any spot weld for which the transmitted maximum values of the loads P, Q and M are known from experiment or global structural analysis. As seen in Fig. 2, the equation of the best fit (mean) curve to all data including LC and HSLA materials is:

$$K_i = 1,223 (N_f)^{-0.187} \quad \text{failure is defined by complete separation.} \quad (6)$$

For 2 and 3 standard deviations (SD) confidence limits, the relationships between  $K_i$  and fatigue life ( $N_f$ ) to separation are:

$$K_i = 621 (N_f)^{-0.187} \quad \text{for 2 SD} \quad (7)$$

$$K_i = 443 (N_f)^{-0.187} \quad \text{for 3 SD} \quad (8)$$

A relationship for the fatigue life of tensile-shear specimens up to the appearance of a crack on its external surface was also determined from experimental results [2,3]: see Fig. 3.

$$K_i = 6,188 (N_f)^{-0.321} \quad \text{failure defined by the appearance of a visible crack.} \quad (9)$$

For 2 and 3 standard deviations (SD) confidence limits, the relationships between  $K_i$  and fatigue life ( $N_f$ ) to the appearance of a crack on its external surface are:

$$K_i = 2,836 (N_f)^{-0.321} \quad \text{for 2 SD} \quad (10)$$

$$K_i = 1,920 (N_f)^{-0.321} \quad \text{for 3 SD} \quad (11)$$

Tables 2 and 3 give simple expressions for the predicted fatigue strength for the DS, TS, and CP spot weld geometries for mean, 2 SD and 3 SD confidence limits based on total complete separation of the spot welded joint. Table 4 summarizes information for tensile-shear spot welds in which the definition of failure is the appearance of a fatigue crack on the external surface.

#### 3.2 Fatigue life ( $N_f$ ) as a function of $K_i$

Another set of best-fit equations, similar to Eqs. 6-11, can be generated for the fatigue life ( $N_f$ ) considering  $K_i$  to be the independent variable:

$$N_f = 1.085e+13 (K_i)^{-3.648} \quad \text{failure is defined by complete separation.} \quad (12)$$

For 2 and 3 standard deviations (SD) confidence limits, the relationships between  $N_f$  (fatigue life to separation) and  $K_i$  are:

$$N_f = 5.4494e+11 (K_i)^{-3.648} \quad \text{for 2 SD} \quad (13)$$

$$N_f = 1.2212e+11 (K_i)^{-3.648} \quad \text{for 3 SD} \quad (14)$$

A relationship for the fatigue life of tensile-shear specimens up to the appearance of a crack on its external surface was also determined from experimental results:

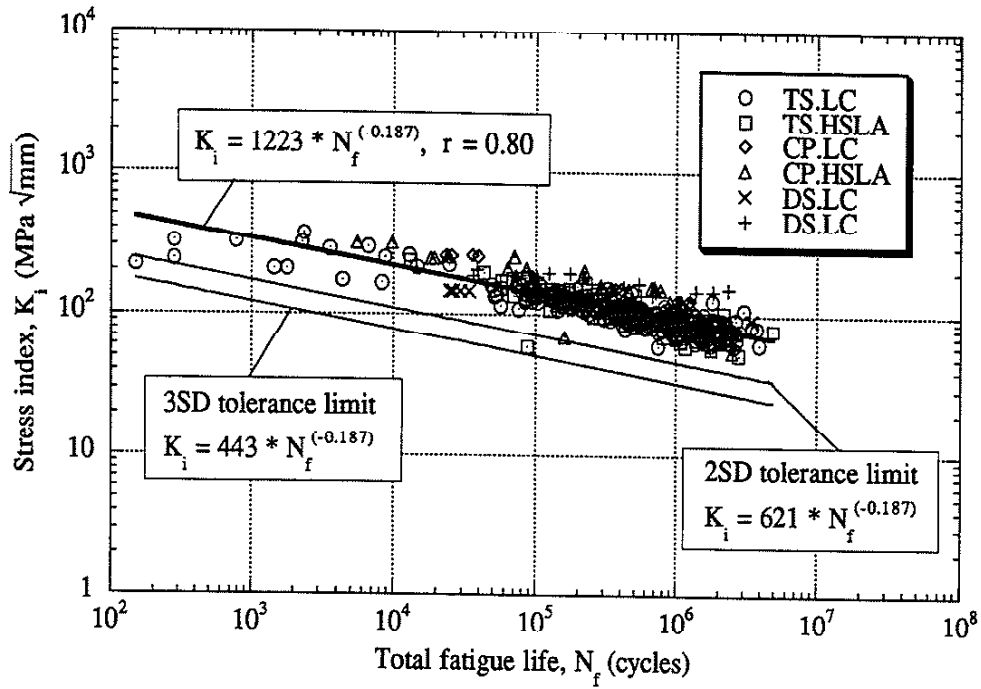


Fig. 2 Correlation between  $K_i$  and fatigue life to separation for all available data for DS, TS, and CP joints [1,2,3].

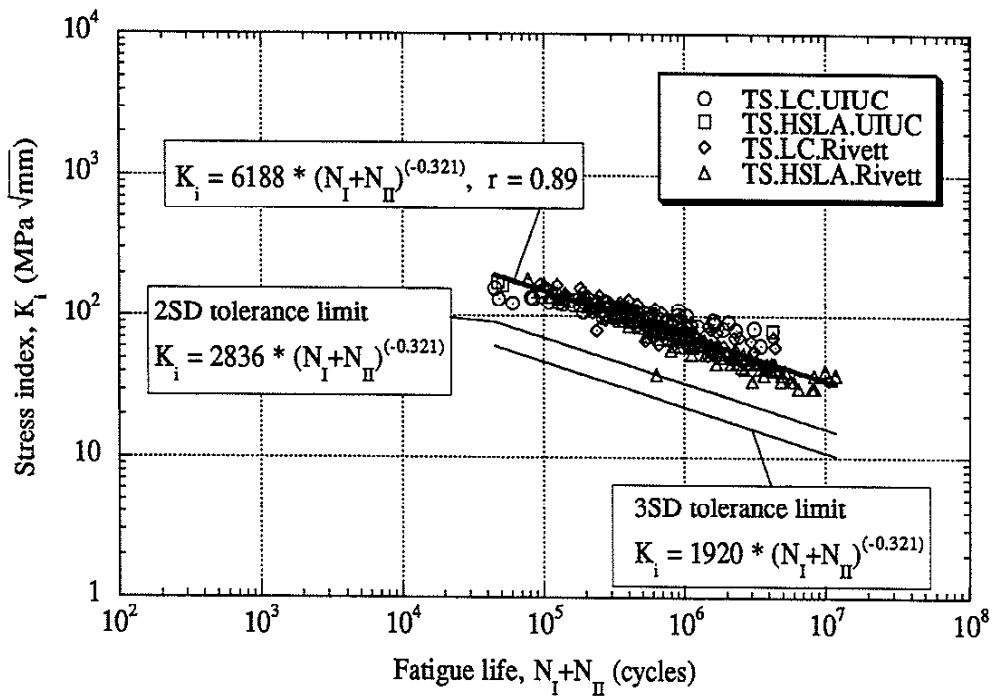


Fig. 3 Correlation between  $K_i$  and fatigue life to appearance of a visible crack for all available data for TS joints [1,2,3].



Table 3

FATIGUE DESIGN FORMULAE FOR HIGH-STRENGTH, LOW-ALLOY (HSLA) STEEL SPOT WELDMENTS (SEPARATION)

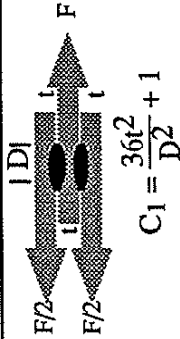
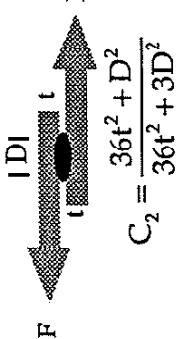
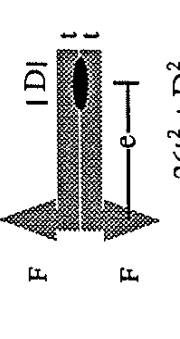


		D=6, W = 38, t = 1.4 mm R = 0	
Geometry	Reliability	Formula	F@10 <sup>5</sup> cycles (N)    F@10 <sup>6</sup> cycles (N)    F@10 <sup>7</sup> cycles (N)
 <p>Double Shear (DS)</p> $C_1 = \frac{36t^2}{D^2} + 1$	<p>mean (50%)    F = 2,825 (1-R)<sup>-0.85</sup> <math>\sqrt{\pi C_1 W}</math> N-0.187</p> <p>2SD (93%)    F = 1,435 (1-R)<sup>-0.85</sup> <math>\sqrt{\pi C_1 W}</math> N-0.187</p> <p>3SD (99%)    F = 1,025 (1-R)<sup>-0.85</sup> <math>\sqrt{\pi C_1 W}</math> N-0.187</p>		8,635    5,615    3,650 4,385    2,850    1,855 3,135    2,035    1,324
 <p>Tensile Shear (TS)</p> $C_2 = \frac{36t^2 + D^2}{36t^2 + 3D^2}$	<p>mean (50%)    F = 2,445 (1-R)<sup>-0.85</sup> <math>\sqrt{\pi C_2 W}</math> N-0.187</p> <p>2SD (93%)    F = 1,240 (1-R)<sup>-0.85</sup> <math>\sqrt{\pi C_2 W}</math> N-0.187</p> <p>3SD (99%)    F = 885 (1-R)<sup>-0.85</sup> <math>\sqrt{\pi C_2 W}</math> N-0.187</p>		3,355    2,180    1,420 1,700    1,105    720 1,215    790    515
 <p>Coach Peel (CP)</p> $C_3 = \frac{36t^2 + D^2}{(6e + D)^2}$	<p>mean (50%)    F = 2,445 (1-R)<sup>-0.85</sup> <math>\sqrt{\pi C_3 W}</math> N-0.187</p> <p>2SD (93%)    F = 1,240 (1-R)<sup>-0.85</sup> <math>\sqrt{\pi C_3 W}</math> N-0.187</p> <p>3SD (99%)    F = 885 (1-R)<sup>-0.85</sup> <math>\sqrt{\pi C_3 W}</math> N-0.187</p>		360    235    155 185    120    75 130    85    55

Table 4

FATIGUE DESIGN FORMULAE FOR LOW CARBON (LC) AND HIGH-STRENGTH, LOW-ALLOY (HSLA) STEEL SPOT WELDMENTS  
(VISIBLE CRACK)<sup>†</sup>

		D = 6, W = 38, t = 1.4 mm R = 0			
Geometry	Reliability	Formula	F@10 <sup>5</sup> cycles (N)	F@10 <sup>6</sup> cycles (N)	F@10 <sup>7</sup> cycles (N)
 $C_2 = \frac{36t^2 + D^2}{36t^2 + 2D^2}$ <p>Tensile Shear (TS)</p>	<p>mean (50%)</p> <p>2SD (93%)</p> <p>3SD (99%)</p>	<p><math>F = 12,375 (1-R)^{-0.85} t \sqrt{\pi C_2 W} N^{-0.321}</math></p> <p><math>F = 5,670 (1-R)^{-0.85} t \sqrt{\pi C_2 W} N^{-0.321}</math></p> <p><math>F = 3,840 (1-R)^{-0.85} t \sqrt{\pi C_2 W} N^{-0.321}</math></p>	4,065	1,940	925
 $C_2 = \frac{36t^2 + D^2}{36t^2 + 3D^2}$ <p>Tensile Shear (TS)</p>	<p>mean (50%)</p> <p>2SD (93%)</p> <p>3SD (99%)</p>	<p><math>F = 12,375 (1-R)^{-0.85} t \sqrt{\pi C_2 W} N^{-0.321}</math></p> <p><math>F = 5,670 (1-R)^{-0.85} t \sqrt{\pi C_2 W} N^{-0.321}</math></p> <p><math>F = 3,840 (1-R)^{-0.85} t \sqrt{\pi C_2 W} N^{-0.321}</math></p>	3,630	1,735	830
			1,665	795	380
			1,125	540	255

<sup>†</sup> The regression analysis of the data in Fig. 3 leads to higher fatigue strength predictions at lives less than 10<sup>5</sup> cycles than those in Tables 2 and 3 in which complete separation at failure is assumed. Thus Table 4 is believed to be correct only for lives greater than 10<sup>5</sup>.

$$N_f = 6.748e+10 (K_i)^{-2.601} \quad \text{failure defined by the appearance of a visible crack.} \quad (15)$$

For 2 and 3 standard deviations (SD) confidence limits, the relationships between  $N_f$  (the fatigue life to the appearance of a crack on its external surface) and  $K_i$  are:

$$N_f = 7.326e+09 (K_i)^{2.601} \quad \text{for 2 SD} \quad (16)$$

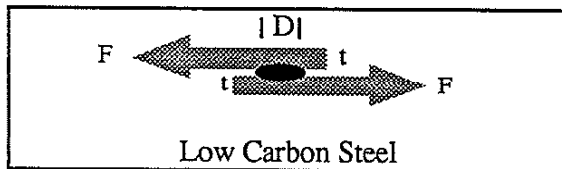
$$N_f = 2.414e+09 (K_i)^{-2.601} \quad \text{for 3 SD} \quad (17)$$

Equations 2 to 5 enable the designer to determine the effect of varying any design parameter on the fatigue performance of the DS, TS, CP and CT joints. The relationship for  $K_i$  (Eq. 1) and the excellent correlation between the value of  $K_i$  and the fatigue life of all available data for spot welds (Eqs. 7 to 17) permit predictions of fatigue life and fatigue strength to be made for any spot weld.

#### 4. EXAMPLE APPLICATIONS OF THE $K_i$ PARAMETER

##### 4.1 Estimating the fatigue life of a tensile-shear (TS) spot weld

A low carbon steel ( $\beta=2$ ) tensile-shear spot weld has a sheet thickness  $t = 1.4$  mm, a nugget diameter  $D = 6.0$  mm, a sheet width or inter-weld spacing  $W = 38$  mm and an applied load range of  $\Delta F = 2,500$  N for a zero to tension load cycle ( $R = 0$ ):



D	=	6.0 mm
t	=	1.4 mm
W	=	38.0 mm
$\beta$	=	2.0
$F_{max}$	=	2,500 N
R	=	0
$N_f$	=	?

The expected (mean) fatigue life to total separation ( $N_f$ ) may be estimated using Eqs. 3 and 12:

$$K_i = \frac{F_{max}}{2t\sqrt{\pi W(36t^2 + D^2)}} \sqrt{36t^2 + D^2} = 94.5 \text{ (N mm}^{-3/2}\text{)}$$

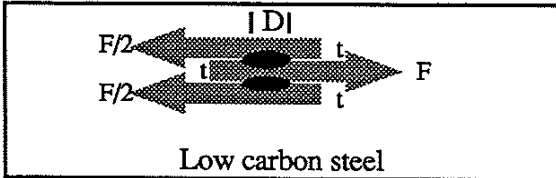
For complete separation

$$N_f = 1.085e+13 (K_i)^{-3.648}$$

$$N_f = \underline{671,000 \text{ cycles}}$$

#### 4.2 Estimating fatigue strength of a double-shear (DS) spot weld

A low carbon steel ( $\beta = 2$ ) double-shear (DS) spot weld has a single sheet thickness  $t = 1.4$  mm, a nugget diameter  $D = 6.0$  mm, a sheet width or inter-weld spacing  $W = 38$  mm is going to be subjected to a zero to tension load cycle ( $R=0$ )



D	=	6.0 mm
t	=	1.4 mm
W	=	38.0 mm
$\beta$	=	2.0
$F_{max}$	=	?
R	=	0
$N_f$	=	$10^5$ cycles

From Table 1 (or Eqs. 2 and 6), the average fatigue strength (50% reliability) at a life (to total separation) of  $N_f = 10^5$  cycles is:

$$F = 3,460 (1-R)^{-0.85} t \sqrt{\pi C_1 W} N^{-0.187} \quad \text{where: } C_1 = \frac{36t^2}{D^2} + 1 \quad (18)$$

$$F = \underline{10,600 \text{ N.}} \quad (50\% \text{ confidence limit})$$

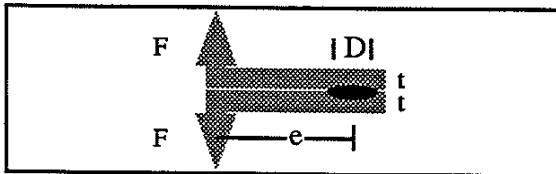
From Table 1 (or Eqs. 2 and 8), the fatigue strength for 99% confidence limit (3 SD) at a life (to total separation) of  $N_f = 10^5$  cycles is:

$$F = 1,255 (1-R)^{-0.85} t \sqrt{\pi C_1 W} N^{-0.187} \quad \text{where: } C_1 = \frac{36t^2}{D^2} + 1 \quad (19)$$

$$F = \underline{3,745 \text{ N.}} \quad (99\% \text{ confidence limit})$$

#### 4.3 Comparing the effects of coach-peel (CP) geometries

A coach-peel spot weld was found to have a actual nugget radius of  $D_a = 4.8$  mm (small) rather than the desired design value  $D_d = 5.8$  mm. Furthermore, the weld nugget was miss-located such that the eccentricity of the load "e" was 31 mm instead of 20.



$D_a$	=	4.8 mm
$D_d$	=	5.8 mm
t	=	1.2 mm
$e_a$	=	31.0 mm
$e_d$	=	20.0 mm

The  $K_i$  for a coach peel joint is:

$$K_i = \frac{F_{max}}{2t\sqrt{\pi W(36t^2 + D^2)}} (D + 6e) \quad (4)$$

For the same fatigue life, that is, keeping  $K_i$  constant and other things being equal:

$$\frac{F_a}{F_d} = \underline{62\%}$$

Equation 4 predicts a reduction in the permissible load range load by a factor of 62% below that desired.

#### 4.4 Influence of coach-peel (CP) flange angle

One remedy for the problem with the coach-peel geometry of Example 2.3 is simply to incline the flange by an angle ( $\theta$ ). Equation 20 below predicts an improvement in the sustained fatigue load to about 83 % of the designed load as a consequence of reducing the flange angle from  $90^\circ$  to about  $48^\circ$ .

$$K_i = \frac{F_{\max}}{2t\sqrt{\pi W(36t^2 + D^2)}} \sqrt{(D + 6e)^2 \sin^2 \theta + \beta D^2 \cos^2 \theta} \quad (20)$$

Figure 4 shows the experimental results for coach-peel specimens having  $90^\circ$  and  $48^\circ$  flank angles; at  $10^6$  cycles, the fatigue strength of the actual ( $q = 90^\circ$ ) and the inclined ( $q = 48^\circ$ ) flange angle joint are 56% and 88% that of the desired design value, respectively.

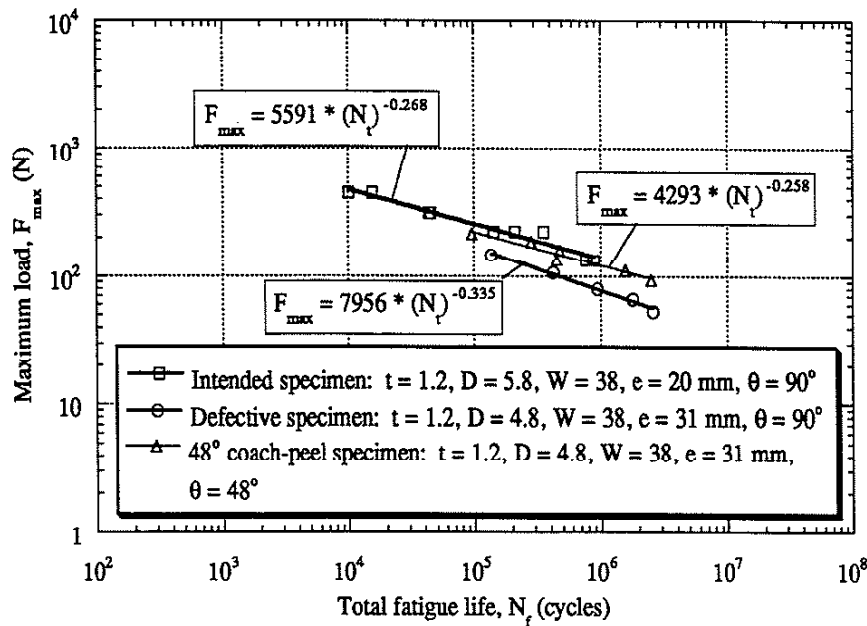


Fig. 4 Maximum applied load versus total fatigue life for design, actual nugget, and actual nugget with an inclined flange ( $\theta = 48^\circ$ ) coach-peel specimens [1].

#### 4.5 Predictions for cross-tension (CT) and sheet-to-tube (STT) components

A variety of tests have been run [1] involving cross-tension (CT) and sheet to tube joints. The geometries of these weldments are shown in Figs. 5. The  $K_i$  values for the tensile shear sheet to



tube (TS-SST) joints were calculated using Eq. 1. The Mode I component was neglected since the rotation of the nugget is limited by the rigidity of the tube. For cases where the sheet thickness was different from the tube thickness,  $K_i$  was calculated using an average sheet thickness of the tube and sheet.

$$K_i = \frac{F}{2r\sqrt{\pi W(36t^2 + D^2)}} D \sqrt{B} \quad (21)$$

For the cross-tension  $K_i$  is given by:

$$K_i = \frac{F}{2r\sqrt{\pi W(36t^2 + D^2)}} (D + 3e) \quad (22)$$

where  $e$  is half the distance from the grip inner edge to the nugget periphery.

The experimental data are plotted in terms of the above  $K_i$  parameters in Fig. 5. Figure 5 contains also some cross-tension (sheet-to-sheet) data. The solid line is the regression analysis mean curve from Fig. 2, i.e., Eq. 6. The agreement between the experimental data and Eq. 6 (solid line in Fig. 5) represents an additional confirmation of the validity of the  $K_i$  parameter as a fatigue design aid.

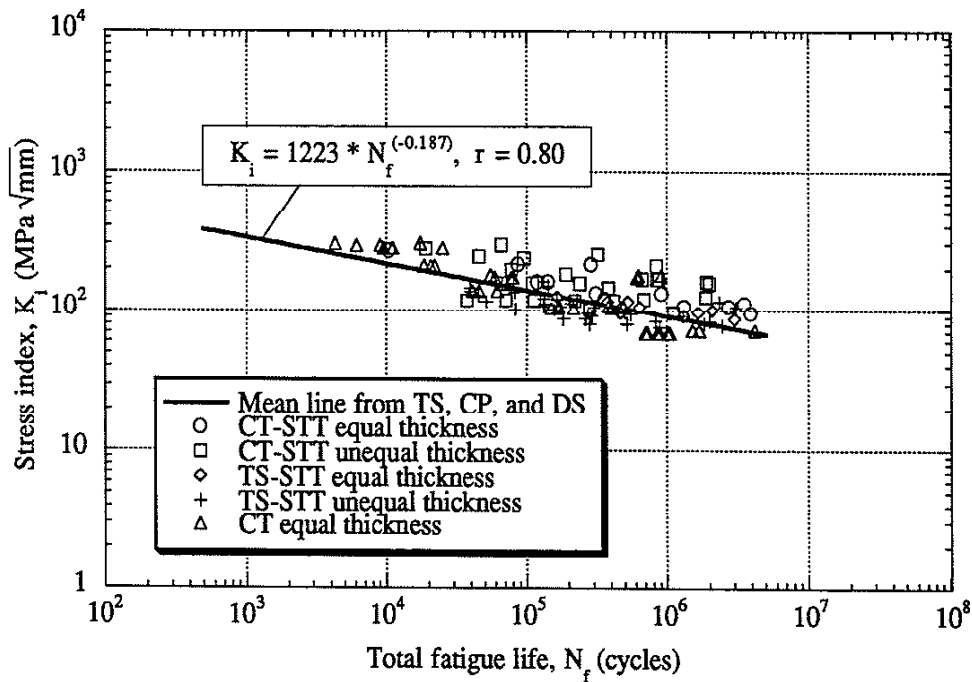
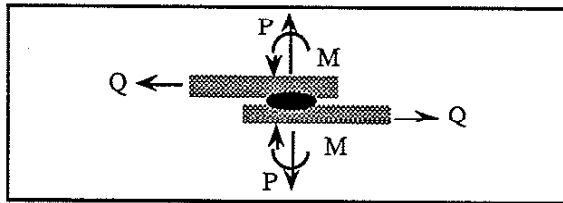


Fig. 5 Stress index ( $K_i$ ) versus life to separation ( $N_f$ ) for the cross-tension and tensile-shear sheet-to-tube (TS-SST and CT-SST) and cross-tension sheet-to-sheet spot welds (CT). The data points represent 120 test records [1]. The solid line is Eq. 6.

#### 4.5 Predictions for a General Spot -Welded Component

In Table 5, the fatigue lives of four, hypothetical spot welds are estimated using Eq. 1.



D	=	5.0 mm
t	=	1.4 mm
W	=	38.0 mm
$\beta$	=	3.0
R	=	0
$N_f$	=	?

#### 5. LIMITATIONS OF THE $K_I$ PARAMETER

The best-fit equations were obtained from fatigue data with total fatigue lives within the range of  $10^4$  to  $10^7$  cycles. Extrapolation of best-fit equations to the low cycle regime ( $N_f < 10^3$  cycles) might overestimate the fatigue life. Likewise, the extrapolation of the best-fit equations beyond  $10^7$  cycles can not account for the situations where the cracks growing through the specimen width may stop and complete separation may never occur. Finally, it should be noted that the  $K_I$  parameter in its current form does not account for the tail effect (contact area behind the nugget) which highly affects the fatigue life of the coach-peel specimens. No situations involving out-of plane shear (Mode III, that is,  $K_{III}$ ) have considered or are included in the data base. Lastly,  $K_I$  does not consider any redundancy in the original structure which may result in a redistribution of stresses in the component.

#### 6. REFERENCES

1. Unpublished spot weld fatigue test data of the authors.
2. Swellam, M. H. and F. V. Lawrence, "A Fatigue Design Parameter for Spot Welds", Fracture Control Program Report No. 157, University of Illinois, (1991).
3. Swellam, M. H., P. Kurath, F. V. Lawrence, "Electric-Potential-Drop Studies of Fatigue Crack Development in Tensile-Shear Spot Welds", Advances in Fatigue Lifetime Predictive Techniques, ASTM STP 1122, M. R. Mitchell and R. W. Landgraf, Eds., American Society for Testing and Materials, Philadelphia, 1992, pp. 383-401.

Table 5

$K_i$  CALCULATIONS AND FATIGUE LIFE ESTIMATES FOR FOUR SPOT WELDS IN A GENERAL, SPOT - WELDED COMPONENT  
 ( $t = 1.4, D = 5, W = 38$  and  $\beta = 3$ )

Spot Weld no.	P (N)	Q (N)	M (N.mm)	$K_{I1} = \frac{P}{D\sqrt{\pi \frac{D}{2}}} + \frac{6M}{D^2\sqrt{\pi \frac{D}{2}}}$ (MPa $\sqrt{\text{mm}}$ )	$K_{II} = \frac{Q}{D\sqrt{\pi \frac{D}{2}}}$ (MPa $\sqrt{\text{mm}}$ )	$K_{eq} = \sqrt{K_{I1}^2 + \beta K_{II}^2}$ (MPa $\sqrt{\text{mm}}$ )	$K_i = \frac{K_{eq}}{G^*}$ (MPa $\sqrt{\text{mm}}$ )	Total Life Eq. 12 (cycles)
1	1,000	1,000	1,000	157	71	200	47	8,622,000
2	2,000	1,000	1,000	228	71	260	61	3,331,000
3	1,000	2,000	1,000	157	143	293	69	2,125,000
4	1,000	1,000	2,000	243	71	272	64	2,796,000

$$* G = \sqrt{\frac{8t^2W}{D^3} \left( \frac{36t^2}{D^2} + 1 \right)}$$